2D Materials

PAPERS

Coupling tension and shear for highly sensitive graphene-based strain sensors

RECEIVED
23 February 2015

REVISED
11 April 2015

ACCEPTED FOR PUBLICATION
14 May 2015

PUBLISHED
25 June 2015

Zenan Qi[1], Jian Zhang[2], Guiping Zhang[3] and Harold S Park[1]

[1] Department of Mechanical Engineering, Boston University, Boston, MA 02215, USA
[2] Microsoft Corporation, 15700 NE 39th St., Redmond, WA 98052, USA
[3] Department of Physics, Renmin University of China, Beijing 100872, People's Republic of China

E-mail: bugubird_zhang@hotmail.com **(G Zhang) and** parkhs@bu.edu **(H S Park)**

Keywords: graphene, strain sensor, electronic transport

Abstract

We report, based on its variation in electronic transport to coupled tension and shear deformation, a highly sensitive graphene-based strain sensor consisting of an armchair graphene nanoribbon (AGNR) between metallic contacts. As the nominal strain at any direction increases from 2.5 to 10%, the conductance decreases, particularly when the system changes from the electrically neutral region. At finite bias voltage, both the raw conductance and the relative proportion of the conductance depend smoothly on the gate voltage with negligible fluctuations, which is in contrast to that of pristine graphene. Specifically, when the nominal strain is 10% and the angle varies from 0° to 90°, the relative proportion of the conductance changes from 60 to ~90%.

Graphene has been proposed for many applications due to its unique physical properties [1–4], in which the electronic transport through the graphene nanoribbon would be affected by a line defect [5]. Of specific interest to the present work, it has been proposed as a strain sensor due to a change in the conductivity of graphene-based materials [6–12]. The field of graphene-based strain sensing has rapidly developed since the experimental observation of the increase in resistance of chemical vapor deposition (CVD) graphene samples when strain is applied in the direction of the electrical current [6]. In order to accurately determine the direction and magnitude of strain, a triaxial graphene-based strain sensor composite was proposed; it was found that the resistance of graphene may be enhanced or reduced by the strain in certain directions [7]. The sensitivity of graphene to strain originates from the deformation of carbon-carbon bonds, which alter the hopping integrals and thus the electronic transport in graphene.

Though the effect of strain on the band structure of graphene and narrow graphene nanoribbons (GNRs) has been widely discussed [13–17], strain sensing based on electronic transport through graphene and GNRs has recently become of wide interest [18–24]. In the present work, motivated by recent experimental findings of the potential benefits of coupled tension/shear deformation to simulate the strain generated due to the movement of human fingers [7], we theoretically study coupled tension and shear deformation on the transport through armchair graphene nanoribbons (AGNR) between metallic contacts.

Most previous theoretical studies of graphene strain sensors have adopted homogeneous junctions. However, no lattice mismatch occurs at the interfaces for homogeneous junctions, whereas the conductance in unstrained GNRs is either zero or one at the Fermi energy $E = 0$ [25]. Unlike most experiments in which the gate voltage is only applied to graphene samples, the Fermi energy E should vary to investigate electronic transport through GNRs. For heterogeneous junctions of GNRs between quantum wire contacts, transport through GNRs is mediated by the gate voltage V_g, as in previous experimental measurement on electrical properties of graphene samples [1–3]. These heterogeneous junctions are inspired by the fact that the contacts are metallic rather than carbon in experiments [1–3] and the conductance of quantum wire contacts is maximal at $E = 0$, because all channels are available to electronic transport.

However, lattice mismatch may exist at the interfaces of heterogeneous junctions. Here we adopt heterojunctions of armchair-edged GNRs between quantum wire contacts, as discussed in [26], to

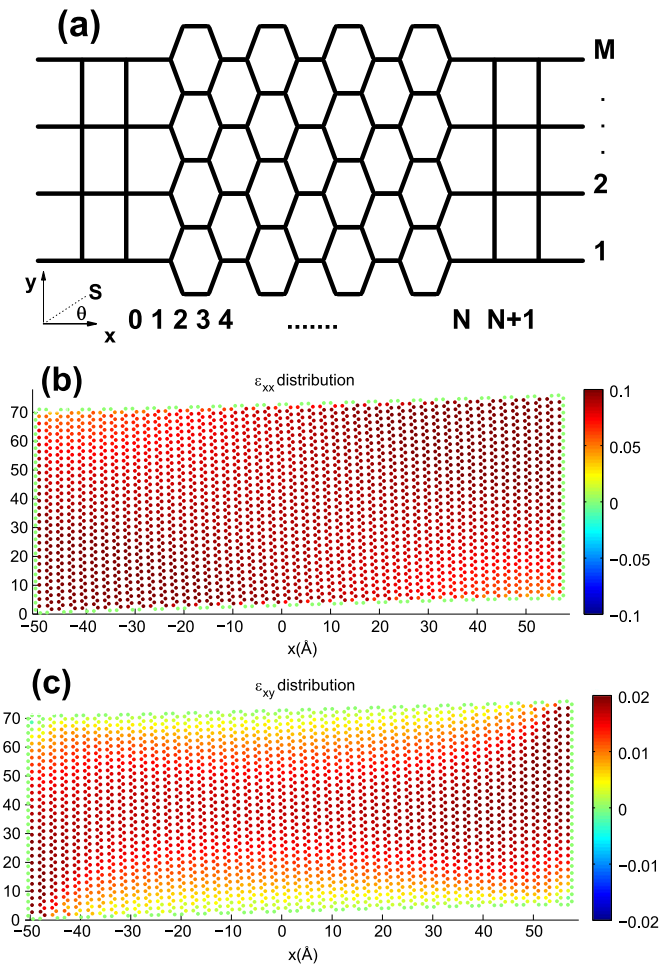

Figure 1. (a) Schematic illustration of the AGNRs connected to two semi-infinite quantum wires. There are N and M carbon atoms in the x and y directions, respectively. θ is the angle between the direction of applied strain S and the x-axis. (b) The tensile and (c) the shear component of the strain at 30° when the nominal strain is $\epsilon_{ns} = 10\%$.

minimize the effect of lattice mismatch at the interfaces and investigate the effect of uniaxial plus shear strain on electronic transport, as illustrated in figure 1. The strain is only applied to the AGNR and impacts the hopping integrals in the AGNR. The Hamiltonian of the AGNR and contacts is described by the tight binding approximation as

$$\hat{H} = \sum_{\langle ij,i'j'\rangle} t_{ij,i'j'}\hat{c}_{ij}^{\dagger}\hat{c}_{i'j'} + V_g \sum_{ij}\hat{c}_{ij}^{\dagger}\hat{c}_{ij}, \qquad (1)$$

where a pair of integers ij indicates the lattice position $\vec{R}_{ij}$, and $\hat{c}_{ij}$ ($\hat{c}_{ij}^{\dagger}$) is the electron annihilation (creation) operator. The summation is over the nearest neighbors indicated by $\langle\cdots\rangle$. $t_{ij,i'j'}$ is the hopping integral between nearest-neighboring sites indexed by ij and $i'j'$. V_g is the effective gate voltage applied to graphene, which is zero in contacts. When V_g slightly varies at the interfaces, the conductance does not change much around $V_g = 0$ [27].

The deformed configurations of the GNRs were obtained by molecular mechanics simulations, where the strain was obtained via applied displacement loading [21, 28]. The rectangular AGNR consisted of 2832 atoms with a length of $L = 10.224$ nm and width $W = 7.018$ nm. Displacements were applied in increments of 0.01Å, followed by a subsequent energy minimization and relaxation until the change in system energy was less than 10^{-7} compared with the previous step. The simulations were performed using the open source package LAMMPS [29] and the AIREBO interatomic potential [30] with a cutoff of 0.68 nm. This potential has been shown to accurately describe carbon-carbon interactions, resulting in accurate predictions of the mechanical properties of graphene [31]. We note that because molecular mechanics simulations were performed, which are intrinsically at 0 K, and because all applied displacements were in-plane, there was no out-of-plane buckling during the simulation.

As shown in figures 1(b) and (c), coupled tension and shear were applied onto AGNRs, and the corresponding strains were calculated, as discussed in previous works [21]. We also define the 'nominal strain' as the displacement applied (regardless of the direction) with reference to the original length. Once the carbon atomic positions are obtained at each value of strain, the hopping along each bond (with the length l)

$V_{pp\pi} = t_0 e^{-3.37(l/a-1)}$ [13] ($t_0 = 2.7$ eV and $a = 0.142$ nm) is used as the basis for the electronic structure and quantum transport calculations. Due to the two-dimensional nature of our analysis, σ bonds were not considered in our calculation.

Strain was applied with a tilted angle θ (figure 1) from 0° to 90° at five different angles, i.e., 0°, 30°, 45°, 60°, and 90°, where 0° loading represents pure tension, 90° represents pure shear, and the other three represent couple tension and shear. To simplify the notation, we also introduce a 'nominal strain' ϵ_{ns}, which is defined as the displacement applied over the original nanoribbon length, regardless of the loading angle. All cases with different loading angles are deformed at three stages, namely, $\epsilon_{ns} = 2.5\%$, 5%, 10%, and we will refer exclusively to ϵ_{ns} in the following. The tension (ϵ_{xx}) and shear (ϵ_{xy}) strain components at the three stages for different loading angles are corresponding as: $\epsilon_{xx} = 2.5\%$, 5%, 10%, and $\epsilon_{xy} = 0\%$, 0%, 0% for 0°; $\epsilon_{xx} = 2.1\%$, 4.1%, 8.7%, and $\epsilon_{xy} = 0.5\%$, 0.9%,1.8% for 30°; $\epsilon_{xx} = 1.6\%$, 3.3%, 7.8%, and $\epsilon_{xy} = 0.7\%$, 1.4%, 2.6% for 45°; $\epsilon_{xx} = 1.1\%$, 2.4%, 7%. and $\epsilon_{xy} = 0.9\%$, 1.8%, 3.1% for 60°; $\epsilon_{xx} = 0\%$, 0%, 0%, and $\epsilon_{xy} = 1.1\%$, 2.2%, 3.7% for 90°. The deformed atomic configuration and the resulting components of the tensile and shear strain at 30° when the nominal strain is $\epsilon_{ns} = 10\%$ is shown in figures 1(b) and (c) [32]. The left contact is fixed, while the right one is shifted with strain similar to reference [9] when the shear strain is present; the hopping integral in contacts and interfaces are not affected by the shear/tension.

At a finite bias voltage V_b, the current transfer from the left contact to the right one is expressed as $I(S, V_b, V_g) = 2e/h \int_{E_f - V_b/2}^{E_f + V_b/2} T(S, E, V_g) dE$ [33], where S refers to the strain and $S = 0$ stands for no deformation in the GNR, e is the electron charge, and h is Planck's constant. $T(S, E, V_g)$ is the transmission at the strain S, the energy E, and the gate voltage V_g. Since the effect of the gate voltage on the strain sensor has been explored in a dual-gate setup [9], we include V_g to estimate the stability and applicability of the graphene-based strain sensor. Based on the tight binding Hamiltonian in equation (1) and the transfer matrix method, the transmission $T(S, E, V_g)$ is obtained through the scattering matrix by solving the Schrödinger equations, which is described in detail in references [35, 36].

$I(S, V_b, V_g)$ at $V_g = 0$ at first increases slowly then sharply with V_b, as shown in figure 2(a). This is because the transmission increases as the GNR deviates from being electrically neutral, which has the lowest density of states [24]. $I(S, V_b, V_g)$ at $V_g = t_0$ at first increases linearly and then sub-linearly with V_b as shown in figure 2(b), since the transmission decreases as the GNR deviates from the highest density of states [24]. The conductance is defined as $G(S, V_b, V_g) = I(S, V_b, V_g)/V_b$, and is directly related to the transmission at Fermi energy $T(S, E_f, V_g)$ at the limit of $V_b \to 0$ [33]. The conductance $G(S, V_b, V_g)$ slightly increases and decreases at $V_g = 0$ and $V_g = t_0$, respectively, when V_b increases, as shown in figure 2(c). When V_g changes, a large oscillation of the conductance at $V_b = 0$ is induced by quantum interference when electrons are reflected at the GNR-contact interfaces [24, 26, 34–36], and electron-hole asymmetry in conductance is originated by odd-numbered rings at the interfaces, as shown in figure 1 [26]. The curve of the conductance versus the gate voltage at $V_b = 0.2t_0$ overlaps the one at $V_b = 0$, and the fluctuation becomes invisible, as shown in figure 2(d), due to the summation of the transmission among the energy range $(E_f - V_b/2, E_f + V_b/2)$.

In strained AGNRs, the transport depends on both the direction and magnitude of the strain S. When the nominal strength of the strain is 10%, the current at both zero and finite V_g is lower than in undeformed AGNR and gradually increases with the change in angle of the applied strain, when the strain varies from 0° to 90° combined with shear, as shown in figures 2(a) and (b). Under pure tension at 0°, the change in the current completely reproduces the observation [6]. The slope of the I-V_b curve (i.e., the conductance) for nearly electrical neutral graphene samples, which corresponds to our result at $V_g = 0$ and which is dependent on the specific experimental setup, is $1.5 \times 10^{-4}\,\Omega^{-1}$ [6] and $2 \times 10^{-5}\,\Omega^{-1}$ [7]. Our results show that the ballistic conductance of the 7.018 nm-wide AGNR is around $3 \times 10^{-5}\,\Omega^{-1}$ and $1 \times 10^{-3}\,\Omega^{-1}$ at $V_g = 0$ and $V_g = t_0$, respectively. The conductance dependence on the strain shown in figure 2(c) is the same as the current dependence on the strain.

We compare the conductance dependence on pure tension and pure shear at 90° to estimate the effect of tension and shear on transport through the AGNR. On one hand, in contrast to the fact that the conductance at $-t_0 < V_g < 0.5t_0$ under pure tension at 90° is higher than undeformed AGNRs as a result of an increase in the hopping integrals along the horizontal direction [24], the conductance under pure shear at 90° is always lower than that in undeformed AGNRs as $|V_g| \geqslant 0.5t_0$, except for some fluctuations, as shown in figure 2. Our calculation is consistent with the observation of the conductance dependence on the shear strain [9]. On the other hand, the conductance around the neutral point (i.e., at small $|V_g|$) increases with the angle of tension/shear as shown in figure 2(c), compared with that under pure tension at 0°. The maximal conductance of undeformed AGNR being MG_0 ($G_0 = 2e^2/h$) occurs at $E = \pm t_0$ and $V_g = 0$ between graphite contacts and at $E = 0$ and $V_g = t_0$ between quantum wire contacts. The maximal conductance of strained the AGNR around $V_g = t_0$

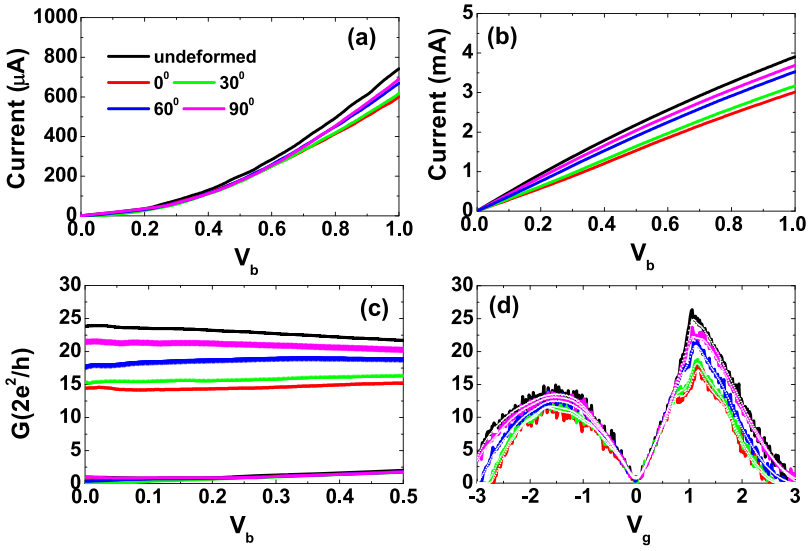

Figure 2. The current through the AGNR depends on the bias voltage V_b at $V_g = 0$ (a) and $V_g = t_0$ (b). The conductance of the AGNR changes with V_b at $V_g = 0$ (lower lines) and t_0 (upper symbols) (c), and with the gate voltage in AGNR at $V_b = 0$ and $V_b = 0.2t_0$ (d). No strain is applied (black line), and the nominal strain ϵ_{ns}, being 10%, is applied at 0° (red line), 30° (green line), 60° (blue line), and 90° (magenta line), respectively. The size of the AGNRs is $M = 29$ and $N = 96$. V_b and V_g in the figures is in the unit of t_0.

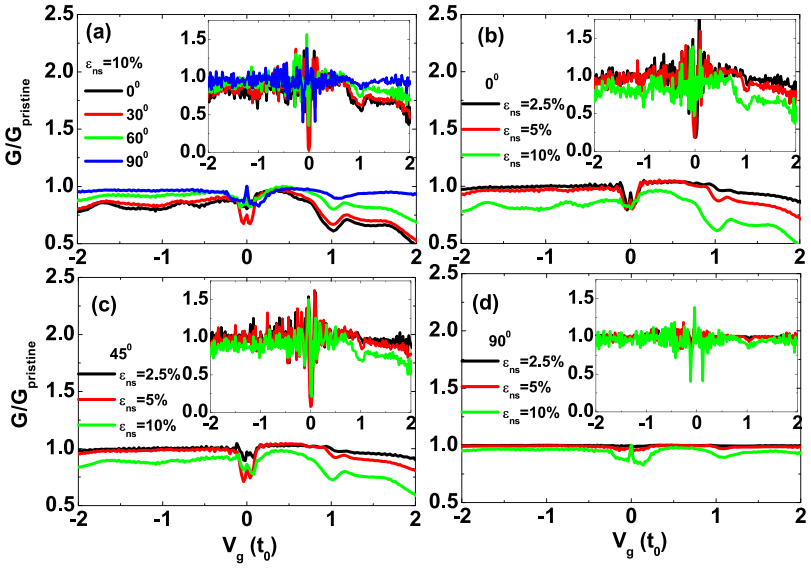

Figure 3. The ratio of the conductance in AGNRs before and after application of the strain with the nominal strain being 10% (a); the nominal strain is 2.5%, 5%, and 10% at an angle of 0° (b), 45° (c), and 90° (d) between the x-axis. The size of the AGNR is $M = 29$ and $N = 96$. The bias voltage is $V_b = 0.2t_0$ (main panels) and $V_b = 0$ (insets).

decreases as a result of deformation in the AGNR when tension and/or shear is applied to the AGNR. The data indicate that electronic transport through the AGNR can be easily mediated by the strain when the system deviates from the electrically neutral region.

In most experiments of graphene-based strain sensors [6, 7], no gate voltage is applied, and graphene may not be electrically neutral due to the doping from metallic contacts [9, 37]. Recently the effect of the gate voltage has been explored [9], and thus we set the gate voltage as a variable parameter to provide information such as the stability of the strain sensor under different gate voltages. The change of current is usually measured under strain, and the percentage of the resistance is used to estimate the effect of the strain on transport through graphene samples [6, 7]. Therefore, we use the ratio of the conductance compared with that in undeformed AGNR, $G(S, V_b, V_g)/G(0, V_b, V_g)$, to measure the sensitivity of the graphene-based strain sensor, as shown in figure 3.

Due to large oscillations in the conductance at $V_b = 0$, a large oscillation is also seen in the ratio $G(S, V_b, V_g)/G(0, V_b, V_g)$, as shown in the insets of figure 3. However, the trends of $G(S, V_b, V_g)/G(0, V_b, V_g)$ are still clear. The

conductance ratio at $V_b = 0.2t_0$, shown in the main panels of figure 3 is relatively smooth at negative gate voltage, shows a large dip or peak around zero gate voltage, and slightly decreases as the gate voltage becomes more positive. When the nominal strain is 10% in figure 3(a), the conductance slightly increases but is smaller than in the undeformed case, as the angle θ varies from 0° to 90°. As θ is varied from 0°, 45°, and 90°, in figures 3(b)–(d) , the conductance decreases as the nominal strain increases from 2.5% to 10%. It is found that the conductance shows little change under pure shear at 90°, as shown in figure 3(d). We demonstrate that this kind of strain sensor is robust, since the relative proportion of the conductance is smooth within a wide gate voltage range [1, 2].

In summary, we have studied a graphene-based strain sensor consisting of an AGNR between metallic contacts in response to combined tension/shear. The conductance and the relative proportion of the conductance decrease as the strain increases. This kind of strain sensor has relatively higher sensitivity to the strength of the strain at finite bias voltage and a wide range of the gate voltage when the strain is parallel to the armchair edge.

Finally, we comment on the performance of a strain sensor made from a zigzag graphene nanoribbon (ZGNR) between quantum wire contacts with a possible lattice mismatch at the interfaces. Compared with the case of the AGNR, the fluctuation of the conductance of the ZGNR is larger when the gate voltage changes. The ratio of the conductance, $G(S, V_b, V_g)/G(0, V_b, V_g)$, ranges between 0.8–1.4 as $|V_g| \leqslant 2t_0$, and the dependence of the conductance ratio on the strain are different from that seen in figure 3 when $|V_g| \leqslant t_0$.

Acknowledgments

HSP and ZQ acknowledge support from the Mechanical Engineering and Physics Departments at Boston University. GPZ thanks support by NSF of China (Grant No. 11204372).

References

[1] Novoselov K S, Geim A K, Morozov S V, Jiang D, Zhang Y, Dubonos S V, Grigorieva I V and Firsov A A 2004 *Science* **306** 666
[2] Novoselov K S, Geim A K, Morozov S V, Jiang D, Katsnelson M I, Grigorieva I V, Dubonos S V and Firsov A A 2005 *Nature* **438** 197
[3] Miao F, Wijeratne S, Zhang Y, Coskun U C, Bao W and Lau C N 2007 *Science* **317** 1530
[4] Schedin F *et al* 2007 *Nat. Mater.* **6** 652–5
[5] Dutta P, Maiti S K and Karmakar S N 2013 *J. Appl. Phys.* **114** 034306
[6] Fu X W *et al* 2011 *Appl. Phys. Lett.* **99** 213107
[7] Bae S H, Lee Y, Sharma B K, Lee H J, Kim J H and Ahn J H 2013 *Carbon* **51** 236
[8] Chun S, Kim Y, Jin H, Choi E, Lee S B and Park W 2014 *Carbon* **78** 601–8
[9] He X *et al* 2014 *Appl. Phys. Lett.* **105** 083108
[10] Wang Y *et al* 2014 *Adv. Funct. Mater.* **24** 4666–70
[11] Souma S, Ohmi Y and Ogawa M 2013 *J. Comput. Electr.* **12** 170–4
[12] Moslemi M R, Sheikhi M H, Saghafi K and Moravvej-Farshi M K 2012 *Microelectron. Reliab.* **52** 2579–84
[13] Pereira V M, Castro Neto A H and Peres N M R 2009 *Phys. Rev.* B **80** 045401
[14] Li Y, Jiang X W, Liu Z F and Liu Z R 2010 *Nano Res.* **3** 545
[15] Peng X, Tang F and Copple A 2012 *J. Phys.: Condens. Matter* **24** 075501
[16] Lu Y and Guo J 2010 *Nano Res.* **3** 189
[17] Sena S H R, Pereira J M Jr, Farias G A, Peeters F M and Costa Filho R N 2012 *J. Phys.: Condens. Matter* **24** 375301
[18] Poetschke M, Rocha C G, Foa Torres L E F, Roche S and Cuniberti G 2010 *Phys. Rev.* B **81** 193404
[19] Wang J Y, Liu Z F and Liu Z R 2012 *AIP Adv.* **2** 012103
[20] Rasuli R, Rafii-Tabar H and Zad A I 2010 *Phys. Rev.* B **81** 125409
[21] Qi Zenan Bahamon D A, Perira Vitor M, Park Harold S and Campbell D K 2013 *Nano Lett.* **13** 2692–97
[22] Bahamon D A and Pereira V M 2013 *Phys. Rev.* B **88** 195416
[23] Cosma Diana A, Marcin M-K, Henning S and Fal'ko V I 2014 *Phys. Rev.* B **90** 245409
[24] Wang J, Zhang G P, Ye F and Wang X Q 2015 *J. Phys.: Condens. Matter* **27** 225305
[25] Peres N M R, Castro Neto A H and Guinea F 2006 *Phys Rev* B **73** 195411
[26] Zhang G P and Qin Z J 2011 *Chem. Phys. Lett.* **516** 225
[27] Wang J, Zhang G P, Ye F and Wang X Q 2015 unpublished
[28] Qi Z, Campbell D K and Park Harold S 2014 *Phys. Rev.* B **90** 245437
[29] http://lammps.sandia.gov
Plimpton S 1995 *J. Comput. Phys.* **117** 1
[30] Stuart S J, Tutein A B and Harrison J A 2000 *J. Chem. Phys.* **112** 6472
[31] Zhao H, Min K and Aluru N R 2009 *Nano Lett.* **9** 3012–5
Wang M *et al* 2012 *Comput. Mater. Sci.* **54** 236–9
[32] Qi Z, Kitt Alexander L, Park Harold S, Pereira Vitor M, Campbell David K and Castro Neto A H 2014 *Phys. Rev.* B **90** 125419
[33] Büttiker M, Imry Y, Landauer R and Pinhas S 1985 *Phys. Rev.* B **31** 6207
[34] Yin Y and Xiong S J 2003 *Phys. Lett.* A **317** 507
[35] Hu S J, Du W, Zhang G P, Gao M, Lu Z Y and Wang X Q 2012 *Chin. Phys. Lett.* **29** 057201
[36] Gao M, Zhang G P and Lu Z Y 2014 *Comput. Phys. Commun.* **185** 856
[37] Giovannetti G, Khomyakov P A, Brocks G, Karpan V M, van den B J and Kelly P J 2008 *Phys. Rev. Lett.* **101** 026803